

Florida Institute of Technology

Scholarship Repository @ Florida Tech

Theses and Dissertations

5-2023

Water-soluble Iron Porphyrin Complex for the Catalytic N-dealkylation of Fentanyl

Amanda Pitt

Follow this and additional works at: <https://repository.fit.edu/etd>



Part of the [Chemistry Commons](#)

Water-soluble Iron Porphyrin Complex for the Catalytic *N*-dealkylation of Fentanyl

by

Amanda Pitt

Bachelor of Science
Chemistry
Florida State University
2021

A thesis submitted to the
Department of Biomedical and Chemical Engineering and Sciences
of Florida Institute of Technology in partial fulfillment of the requirements for the
degree of

Master of Science
in
Chemistry

Melbourne, Florida
May 2023

We the undersigned committee hereby approve the attached thesis,
“Water-soluble Iron Porphyrin Complex for the Catalytic *N*-dealkylation of Fentanyl.”

by
Amanda Pitt

Jessica Smeltz, Ph.D.
Assistant Professor
Biomedical and Chemical Engineering and Sciences
Major Advisor

Bo Wang, Ph.D.
Assistant Professor
Biomedical and Chemical Engineering and Sciences

Rudolf Wehmschulte, Dr. rer. nat.
Professor
Biomedical and Chemical Engineering and Sciences

Manolis Tomadakis, Ph.D.
Professor and Department Head
Biomedical and Chemical Engineering and Sciences

Abstract

Water-soluble Iron Porphyrin Complex for the Catalytic *N*-dealkylation of Fentanyl

Author: Amanda Pitt

Advisor: Jessica Smeltz, Ph.D.

An increase in the misuse of opioids in the United States and the increasing potency of analogs necessitates novel treatments of opioid overdose. The chemical structure of synthetic opioids, such as fentanyl, carfentanil, and morphine possess a trialkyl amine functional group (-NR₃) which makes for a promising target for potential catalysts. Iron (III)-tetrasulfonatophenyl porphyrin (complex **9**) was synthesized as a potential catalyst for degradation of fentanyl. Complex **9a** was prepared from the direct reaction of the free porphyrin and FeSO₄. Complex **9b** was prepared from the direct reaction of the free porphyrin and FeCl₂ in refluxing DMF. The complexes were characterized using UV-vis spectroscopy. We hypothesized that, because the structure of complex **9** is similar to that of cytochrome P450, an enzyme found in the liver, complex **9** would be capable of catalytically degrading fentanyl. The catalytic activity of complex **9** was assessed in aqueous conditions at 37°C with varying concentration of fentanyl and the removal of fentanyl was determined using high resolution mass spectrometry. Complex **9a** was found to remove 30.75% of fentanyl from solution after 72 hours with a catalyst to substrate ratio of 5:1. Most notably, a breakdown product observed following this reaction is norfentanyl, an

inactive fentanyl analog that is formed via the *N*-dealkylation of fentanyl at the piperidine ring. Complex **9b** was found to remove 96.71% of fentanyl from solution after 72 hours with a catalyst to substrate ratio of 5:1. No breakdown products were observed for this reaction.

Table of Contents

Abstract.....	iii
Table of Contents.....	v
List of Tables.....	vii
List of Figures.....	viii
List of Schemes.....	ix
Acknowledgements.....	x
Chapter 1: Introduction.....	1
1.1 The Use and Misuse of Opioids.....	1
1.2 Threat of Fentanyl as a Chemical Weapon.....	2
1.3 Metalloporphyrins in Biology and Catalysis.....	4
1.3.1 Metalloporphyrins in Biology.....	4
1.3.2 Metalloporphyrins in Oxidative Catalysis.....	7
1.4 Alternative Methods for the Degradation of Fentanyl.....	10
1.5 <i>N</i> -dealkylation of Amines.....	12
1.5.1 Transition Metal Catalyzed <i>N</i> -dealkylation.....	13
1.6 Hypothesis and Overview of Experimental Objectives.....	18
Chapter 2: Degradation of Fentanyl Using Tetra(<i>p</i>-sulfonatophenyl)porphyrin Iron (III).....	20
2.1 Introduction.....	20
2.2 Results.....	25
2.2.1 Synthesis and Characterization of Iron (III) Porphyrins.....	25

2.2.2	Degradation of Fentanyl in Aqueous Solutions Using Complex 9a ...	25
2.2.3	Degradation of Fentanyl in Aqueous Solutions Using Complex 9b ...	28
2.3	Discussion.....	28
2.3.1	Characterization and Purification of Iron Porphyrin Complexes.....	28
2.3.2	Removal of Fentanyl Using Complex 9a	31
2.3.3	Removal of Fentanyl Using Complex 9b	32
2.4	Conclusions.....	32
2.5	Materials and Methods.....	33
2.5.1	General Data.....	33
2.5.2	Synthesis of (TSPP)Fe(III).....	34
2.5.3	Synthesis of (TSPP)Fe(III).....	34
2.5.4	Degradation Studies Performed with Complex 9a	35
2.5.5	Degradation Studies Performed with Complex 9b	35
	Conclusions.....	36
	Future Work.....	37
	References.....	38

List of Tables

Table 1.	Products observed following breakdown of fentanyl using complex	
9a	29

List of Figures

Figure 1.	Fentanyl metabolites following breakdown by CYP 3A4.....	6
Figure 2.	General structure of (a) first generation, (b) second generation, and (c) third generation metalloporphyrin, where X is an electron withdrawing group and Y is a halogen atom.....	8
Figure 3.	Fentanyl metabolites following breakdown via strong oxidizers identified on LC-MS.....	11
Figure 4.	Structure of fentanyl; (1): phenethyl ring, (2): piperidine ring, (3): carbamide, (4): phenyl ring.....	17
Figure 5.	General structure of water-soluble metalloporphyrin.....	19
Figure 6.	FeTSPP catalyzed epoxidation and hydroxylation.....	23
Figure 7.	UV-visible spectrum of 9a	26
Figure 8.	Calibration plot of 9a following purification on ion-exchange column.....	26
Figure 9.	UV-visible spectrum of 9b	27
Figure 10.	Calibration plot of 9b following purification on Sephadex column....	27
Figure 11.	Change in fentanyl peak area at varying catalyst substrate ratios from time 0 to 72 hours, using complex 9a	29
Figure 12.	Proposed breakdown products for the degradation of fentanyl in aqueous solutions.....	30
Figure 13.	Change in fentanyl peak area at varying catalyst substrate ratios from time 0 to 72 hours, using complex 9b	30

List of Schemes

Scheme 1.	Proposed mechanism for the <i>N</i> -dealkylation of tertiary amines by (TSPP)Rh(III).....	17
Scheme 2.	Equilibrium of monomeric and dimeric forms of FeTSPP.....	21

Acknowledgements

I would like to thank Dr. D. Andrew Knight for his guidance and support throughout this project. I would also like to thank Dr. Clemence Queffelec for her guidance. Additionally, I would also like to acknowledge my committee members, Dr. Rudolph Wehmschulte and Dr. Bo Wang. I would also like to acknowledge the chemistry department and Florida Institute of Technology and the Defense Threat Reduction Agency for funding my research. Finally, I would like to thank Anneli, Deneyelle, Hemant, and the rest of the Knight Group for their support.

Chapter 1 Introduction

1.1 The Use and Misuse of Opiates and Opioids

Opiates have been in use since ancient times recreationally, as well as for medical purposes, due to their analgesic and anesthetic properties.¹ The term opiates refers to the chemicals extracted from opium, which is found in the poppy plant *Papaver somniferum*.² Commonly used opiates include morphine and codeine.

Currently, in the United States, there exists a crisis concerning the misuse of opioids. It is estimated that the United States, which constitutes about 5% of the global population, accounts for roughly 80% of opioid consumption globally.² Opioids differ from opiates in that opioids are synthetic compounds with analgesic and anesthetic properties similar to morphine. Common opioids include meperidine, tramadol, fentanyl, and fentanyl derivatives such as carfentanil and alfentanil.² According to the National Institute on Drug Abuse (NIDA), 68,630 of the 91,799 drug-involved overdose deaths in 2020 in the United States involved opioids.³ Fentanyl (**1**) (Figure 1), an opioid with a potency 100 times greater than morphine, is the subject of increasing concern among public health officials, as the misuse of fentanyl has grown rapidly over recent years.

First synthesized from pethidine by Janssen Pharmaceuticals in the 1960s, fentanyl is widely used in clinical practice due to its use as a short-acting intravenous (IV) anesthetic. Because fentanyl does not cause histamine release and generally has

fewer adverse cardiovascular effects than morphine, it is often preferred over morphine in certain clinical settings. Fentanyl can also be introduced into the body via transdermal patches, buccal lozenges, and intranasal spray for patients who require long-acting pain-relief. Fentanyl has a high lipid solubility, which allows for the drug to enter the brain quickly, producing analgesic effects in under 5 minutes via IV injection.²

The current state of the art in the treatment of opioid overdose is naloxone. Naloxone effectively reverses the effects of fentanyl in the human body by functioning as an opioid antagonist, competing with, and ultimately displacing, the receptor-bound opioid. Once the opioid is displaced from the receptor, it is then removed from the body naturally, via the oxidation by iron-containing cytochrome P450 enzyme present in the liver. Although fentanyl is extensively metabolized in the liver, a small percentage of the opioid is excreted through urine.⁴ While this method has proven to be effective, it is not without drawbacks. Because naloxone binds to the μ -opioid receptor, withdrawal symptoms can be induced. Additionally, if the opioid is particularly potent, such as carfentanyl, repeated dosing of naloxone may be required to sufficiently reverse the symptoms of overdose. If a patient is a habitual opioid user, new opioid receptors can be expressed, rendering naloxone ineffective.⁵

1.2 Threat of Fentanyl as a Chemical Weapon

Fentanyl is classified as a pharmaceutical based agent. Pharmaceutical based agents (PBAs) are chemical substances with pharmaceutical applications that, in cases of overexposure, can cause incapacitation or death.² The increasing potency of fentanyl and its many analogs not only poses a public health risk to individuals, but law enforcement and counter-terrorism officials fear that there is also a risk of accidental or deliberate exposure to fentanyl for large populations and war fighters. This fear is not without precedent.

On October 23, 2003, Chechen rebels entered a Moscow theater, taking around 900 civilians hostage. After fifty-seven hours, Russian Special Forces deployed an aerosolized gas into the theater to neutralize the terrorists. The gas incapacitated the occupants and first responders had access to an antidote to reverse the effects of this gas for the hostages but did not possess enough medical personnel to administer the antidote to every hostage. This oversight led to the death of at least 129 civilians and the hospitalization of 245 civilians.² The exact chemical components of the gas remained unknown until an analysis of the clothing from a theater occupant was obtained. It was discovered that the aerosolized gas contained carfentanil and remifentanil, both of which are derivatives of fentanyl with potencies of 100 times and 10,000 times greater than morphine, respectively.⁶

Fentanyl has many analogs, which often have far greater potency than fentanyl itself. These analogs can be synthesized cheaply, often by rogue chemists, and added to other narcotics, such as heroin, which leads to a sharp increase in accidental deaths associated with opioids. Many fentanyl analogs are novel, with unknown toxicity and potency.² Because of this, exposure to an extremely potent fentanyl analog could pose a challenge for first responders aiming to administer antidotes within a sufficient timeframe. Additionally, the lethal dose for certain fentanyl analogs, such as carfentanil, is small. A lethal dose of carfentanil is between 2 μg and 20 μg , meaning a small amount could, in theory, kill many people.² As such, there exists a need for a rapid, widely available antidote that could reverse the lethal effects of fentanyl and its analogs.

1.3 Metalloporphyrins in Biology and Catalysis

1.3.1 Metalloporphyrins in Biology

Porphyrins are a class of highly conjugated macrocycles consisting of four pyrrole units linked together by methine bridges and resonance structures lend stability to the porphyrinic ring. Porphyrins are naturally occurring compounds, but synthetic porphyrins have been obtained for use in catalysis, medicine, and electronics.⁷ Naturally occurring porphyrins include chlorophyll, which aids in photosynthesis, and Heme B, which carries oxygen throughout the body.⁷

More generally, the class of heme enzymes found in both eukaryotic and prokaryotic organisms are known as cytochromes P450 (CYP).⁸ CYPs, which contain an iron porphyrin active site, participate in vital life processes, including the oxidation of endogenous and exogenous compounds. These include steroids, pollutants, and pharmaceuticals.⁸

CYPs are divided into families and subfamilies, with the human body containing 18 families and 42 subfamilies.⁹ The most abundant CYP isoform expressed in the human body is CYP 3A4, which is mostly expressed in the liver and gastrointestinal tract. A feature of CYP 3A4 is its lowered substrate specificity, which renders the enzyme available to metabolize a diverse group of chemicals, regardless of size or structure.⁸

The majority of CYPs are monooxygenases capable of performing regioselective and stereoselective oxidation of substrates. For monooxygenase function *in vivo*, redox partner systems are required. Most CYPs use NADPH driven redox partner systems.¹⁰

The degradation of fentanyl in the body occurs via hepatic metabolism. CYP 3A4 is believed to be the principal enzyme involved in the metabolism of fentanyl. The breakdown of fentanyl is accomplished via an *N*-dealkylation of the piperidine ring

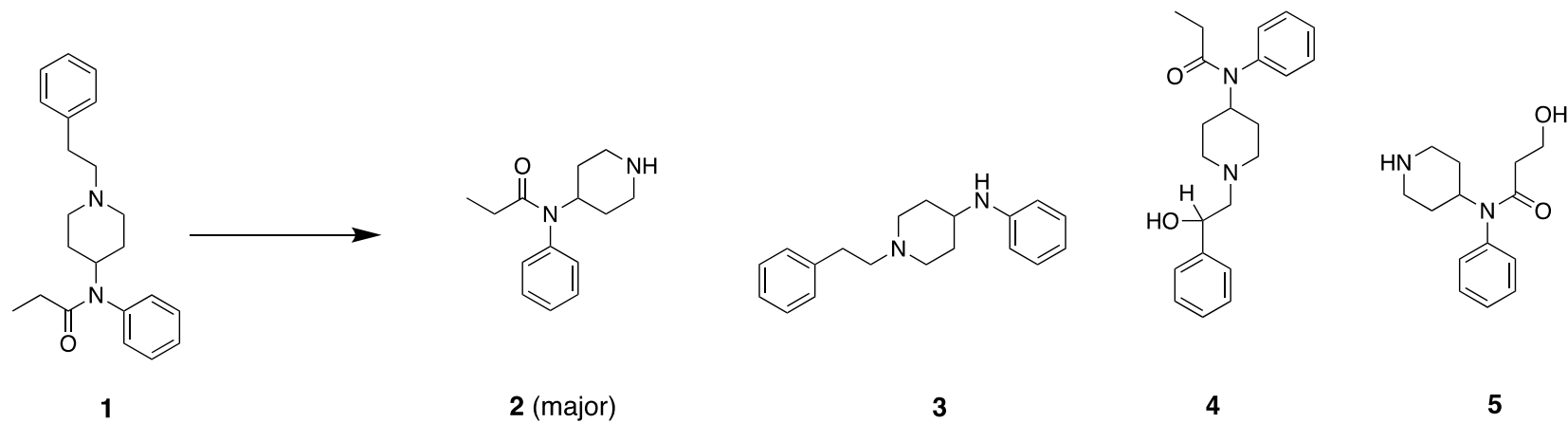


Figure 1. Fentanyl metabolites following breakdown by CYP 3A4.

yielding a major product of norfentanyl (**2**).¹¹ Other metabolites include despropionylfentanyl (**3**), hydroxyfentanyl (**4**), and hydroxynorfentanyl (**5**) (Figure 1).

1.3.2 Metalloporphyrins in Oxidative Catalysis

Due to the reactivity of metalloporphyrins in biological systems, researchers have been exploring the use of synthetic metalloporphyrins for the oxidative catalysis of a variety of substrates. The use of synthetic metalloporphyrins was first reported in the 1970s by Groves *et al.*, which discussed the use of an iron porphyrin as a catalyst for the epoxidation of alkenes. Since then, the synthetic routes of these porphyrins have been developed in order to enhance the catalytic activity. The structures of the metalloporphyrins can be divided in three generations. The first generation of metalloporphyrins consists of a metal center coordinated to a tetraphenyl porphyrin. The second generation introduces electron-withdrawing groups, such as halogen atoms. The second-generation porphyrins have enhanced catalytic performance compared to the first generation due to the increased electrophilicity and oxidizing power of the catalytic intermediate species. The third generation of metalloporphyrins feature the introduction of bulky groups to the β -pyrrole rings of the porphyrin. The structures of porphyrins from each generation are shown in Figure 2. The third generation does not perform as well as the second generation, as researchers have found that the metalloporphyrins in the third generation undergo inactivation, resulting in poor catalytic yield.

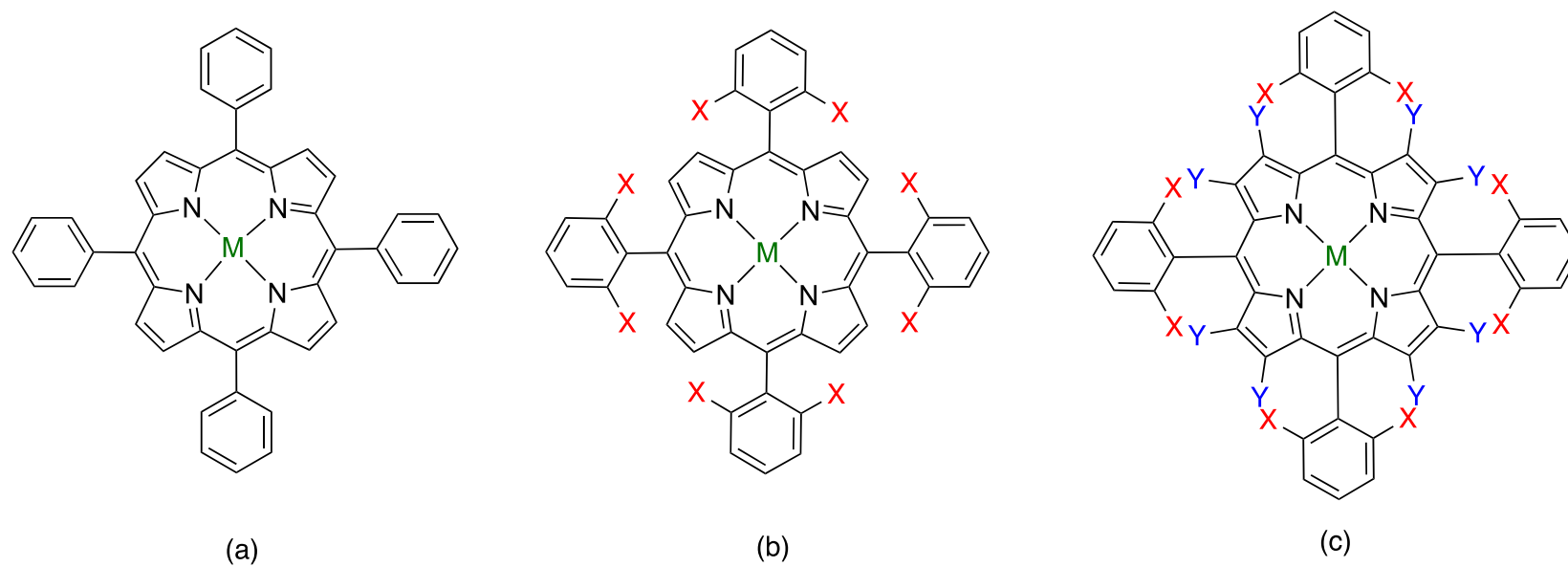


Figure 2. General structure of (a) first generation, (b) second generation, and (c) third generation metalloporphyrin, where X is an electron withdrawing group and Y is a halogen atom.

Since Groves *et al.* reported the use of a first generation [Fe(TPP)]Cl as a catalyst for the epoxidation of *cis*-stilbene and hydroxylation of adamantane in the presence of PhIO, extensive research has been conducted using metalloporphyrin complexes as catalyst for a wide variety of reactions. Wang *et al.* reported the use of *meso*-tetra(*p*-methoxyphenyl)porphyrin and *meso*-tetra(*p*-nitrophenyl)porphyrin complexes with Fe(III), Mn(III), or Co(III) metal centers for the oxidation of *p*-cresol. It was discovered that the porphyrin with the methoxy substituent showed higher catalytic activity, regardless of the metal center, than the porphyrin with the nitro substituent. Additionally, Wang *et al.* found that the formation of *p*-hydroxybenzaldehyde was selective dependent on the metal center of the porphyrin, with Co(III) having the highest selectivity, at 60%, with Fe (III) and Mn(III) 37% and 45% respectively. The researchers theorize that the use of the Co(III) porphyrin may involve an auto-oxidation process while the use of Fe(III) and Mn(III) porphyrins may preferentially form the oxo-metal(IV) porphyrin cation radical.¹²

Guo *et al.* reported the use of a tetraphenyl porphyrin with a Co(III) metal center for the aerobic oxidation of cyclohexane on the industrial scale. The researchers used a low concentration of catalyst, 200 μ M at 145 °C. It was found that, compared to non-catalyzed cyclohexane oxidation with air, catalyzed reactions occur at a lower temperature, 145 °C for catalyzed and 165 °C for non-catalyzed. Additionally, it was found that this reaction significantly increases the low conversion rates and the low yields that often occur during the oxidation of cyclohexane on the

industrial scale. The cyclohexane conversion rate increased from 4.8% to 7.1% and the cyclohexanone yield increased from 77% to 87%.¹²

1.4 Alternate Methods for the Degradation of Fentanyl

Research into alternative methods for the degradation of fentanyl is active and growing. A study conducted by Qi et al. reported that the degradation of fentanyl occurs in the presence of strong oxidizers and hypochlorites. The researchers found that the oxidative *N*-dealkylation of fentanyl at the piperidine ring is the main metabolic pathway that occurs in peroxide.⁴ The *N*-dealkylation can also occur at the amide present in fentanyl. The structures of the metabolites were determined using LC-MS and based on retention times and $M \pm H^+$ peaks (Figure 3). Norfentanyl is an inactive analog of fentanyl, making the oxidative *N*-dealkylation at the piperidine ring the ideal pathway for decontamination. Fentanyl has also been shown to degrade in the presence of a strong acid or heat.¹³ Garg, et al. studied the degradation of fentanyl in various conditions; thermal degradation, oxidation degradation, acid/base degradation, and photodegradation. In the case of thermal degradation, fentanyl was heated in a glass tube for five minutes at 350°C. Five fentanyl degradants were detected using HPLC, two known degradants and three unknown degradants, with norfentanyl identified as one of the degradants. Fentanyl was mixed with 0.3% hydrogen peroxide and analyzed at various time points to determine if fentanyl can be degraded in the presence of an oxidizer. It was found that approximately 10% of fentanyl was degraded after 24 hours. In the presence of 5M HCl at 70°C,

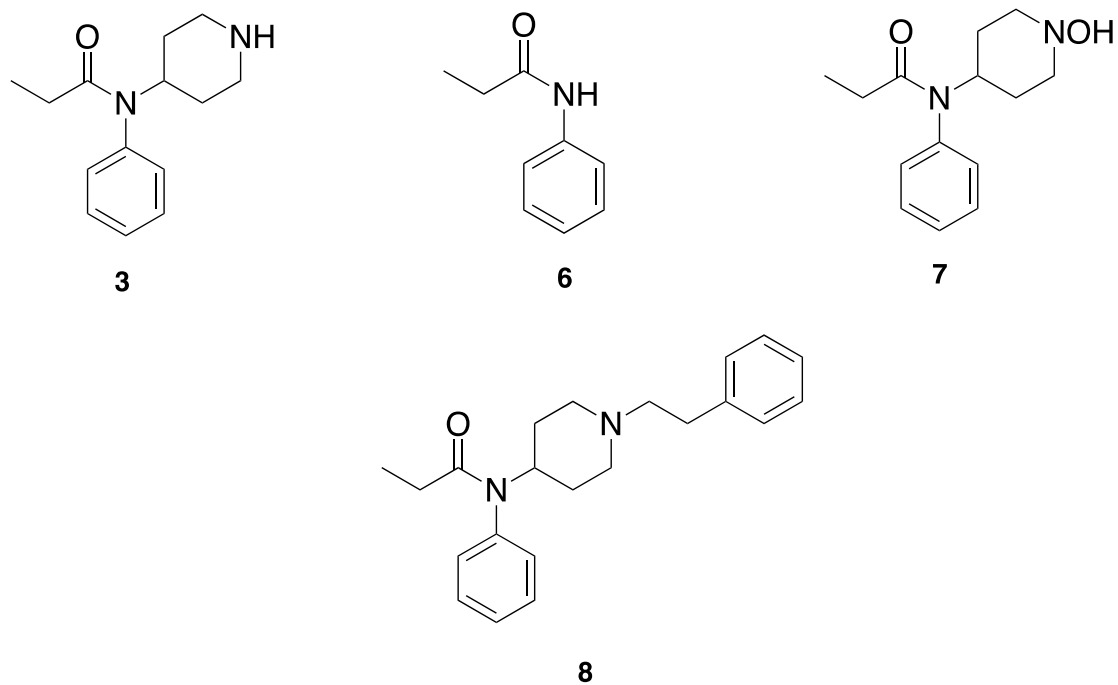


Figure 3. Fentanyl metabolites following breakdown via strong oxidizers identified on LC-MS.

approximately 35% of fentanyl decomposed, selectively producing N-phenyl-1-(2-phenylethyl)-piperidin-4-amine, which is the expected product following acid catalyzed hydrolysis.¹³ In the presence of 5 M NaOH at 70 °C, no degradants, known or unknown, were detected. Additionally, Garg et al. exposed fentanyl to UV light at 365 nm and white fluorescent light for seven days and found that fentanyl was very stable to light and did not degrade after exposure.¹³

The photodegradation of fentanyl has been found to occur with a xenon lamp in the presence of catalysts TiO₂ or ZnO.¹⁴ Trawiński et al. studied the photodegradation of fentanyl in pure water samples and river water samples by exposing the samples to a xenon lamp. Similar to the findings produced by Garg et al., it was found that fentanyl is photostable and does not degrade in the presence of light only. The half-life ($t_{1/2}$) of fentanyl in pure water was determined to be over 1,000 minutes. In the river water matrix, $t_{1/2}$ was found to be much lower but still quite long, at around 138 minutes. Trawiński et al. introduced TiO₂ or ZnO to both the pure water samples and river water samples at loading rates of 100, 200, and 300 mg/L. It was found that TiO₂ was the more effective catalyst of the two, completely degrading fentanyl in pure water in just 16 minutes, with a $t_{1/2}$ less than two minutes, compared to ZnO at 300 mg/L, $t_{1/2}$ is around seven minutes.¹⁴

1.5 *N*-dealkylation of Amines

More broadly, research into various methods to successfully *N*-dealkylate tertiary amines in general is quite comprehensive, given the ubiquity of the carbon-nitrogen bond in various organic molecules and biomolecules. The cleaving of the C-N bond via *N*-dealkylation in vivo is an important metabolic pathway for pharmaceutical compounds containing amine groups. These reactions are catalyzed by the CYP family of enzymes. Furthermore, the *N*-dealkylation of tertiary amines has applications beyond biological applications, including in fine chemicals and agrochemicals because of the synthetic value of *N*-dealkylated amines.¹⁵

One of the oldest methods for the *N*-dealkylation of amines is the von Braun method, first reported in 1900. In general, the von Braun method consists of a reaction between a tertiary amine and a cyanogen bromide, which yields the bromide salt of the quaternary cyanoammonium intermediate complex. The cyanoammonium intermediate forms a cyanamide, which yields a secondary amine following acid or base hydrolysis. This is true for acyclic amines. For cyclic amines, a ring opening may occur, leading to the formation of a long-chain bromo-alkyl cyanamide, however, the preferred pathway is the removal of the methyl group attached to the ring nitrogen.¹⁵

1.5.1 Transition-metal catalyzed *N*-dealkylation

Transition-metal catalyzed *N*-dealkylation of amines has been widely studied and employed. For the large-scale *N*-demethylation of opioid alkaloids, Pd-catalyzed *N*-demethylation has been extensively used by pharmaceutical companies. In 1979, Murahashi et al. reported the use of palladium black to catalyze the hydrolysis of aliphatic and cyclic tertiary amines in the presence of HCl, with a catalyst to substrate ratio of 40%.¹⁶ Murahashi et al. also reported that the use of PdCl₂ and Pd(OAc)₂ as catalysts yielded similar results. The *N*-demethylation of hydrocodone to norhydrocodone was reported by Carroll et al. and is the first report of a Pd-catalyzed *N*-demethylation of an opiate. Norhydrocodone was obtained in 40% yield. The researchers attempted this reaction with other opiates such as oxycodone, codeine, or morphine but found that the reaction only proceeded for hydrocodone.¹⁷

Iron catalyzed *N*-dealkylation reactions are widely studied due to the desire to simulate the CYP-catalyzed *N*-dealkylation that occurs in vivo. Santa et al. reported the use of an iron porphyrin [Fe(III)TPPCl] in the presence of O₂ for the oxidative *N*-dealkylation of various tertiary amines at room temperature with a catalyst loading rate of one mol%. The reactions were completed at analytical scale and yielded secondary amines.¹⁸ Similarly, Do Pham et al. used Fe(III)-TAML (tetra-amidato-macrocyclic ligand) as a catalyst for the oxidative *N*-demethylation of tropane alkaloids atropine and scopolamine. These reactions were completed at room temperature and at the preparative scale, yielding noratropine and norscopolamine

with only a one mol% catalyst loading rate. An advantage to this reaction is the products can be isolated in high purity via liquid-liquid extraction, eliminating the need for chromatographic purification. This research has great importance in the development of pharmaceuticals, as noratropine and norscopolamine are key in the synthesis of the bronchodilators.¹⁹ Furthermore, Dong *et al.* reported the use of Fe(II)TSPPCl for the oxidative *N*-demethylation of codeine. It was found that norcodeine, the inactive metabolite of codeine, was produced in 91% yield after 72 hours with a 0.3 molar equivalent of catalyst. When the catalyst to substrate ratio was altered to a one-to-one ratio, norcodeine was produced in 44 hours with an 87% yield. A key finding in the study conducted by Dong *et al.* was the recyclability of the catalyst, producing nor metabolites of the opiate alkaloids in consistently high yields for four cycles.²⁰

Additionally, the degradation of tertiary amines in general has been extensively studied in various conditions, such as in the presence of $\text{Cu}(\text{OAc})_2 \cdot \text{H}_2\text{O}$ at 100°C , as shown by research completed by Wang *et al.*²¹ Typically, the *N*-dealkylation of tertiary aromatic amines requires the use of *N*-formylating agents, which yield *N*-arylformamides. *N*-arylformamides have extensive applications in organic synthesis and have shown potential for biological activities. As such, there has been extensive research into developing novel routes for synthesis. Wang *et al.* developed a novel method for the $\text{Cu}(\text{OAc})_2 \cdot \text{H}_2\text{O}$ catalyzed *N*-dealkylation and oxidation of *N*-methyl using *N,N*-dimethylaniline as the substrate in the presence of TEMPO (2,2,6,6-tetramethylpiperidine 1-oxyl) and oxygen. It was found that *N*-phenylformamide was

produced in 77% yield when reacted with 10 mol% of $\text{Cu}(\text{OAc})_2 \cdot \text{H}_2\text{O}$ and 3 equivalents of TEMPO.²¹

While the information gleaned from these studies provides insight into mechanisms of fentanyl degradation, the application of these studies does not entirely extend to biological applications due to the extreme conditions in which these studies are performed and lack of biocompatibility of the materials. As such, research into a catalyst that models the CYP 3A4 enzyme in the liver is ideal. In order to accomplish this, it is important to understand how opioids interact with enzymes and receptors in the human body, specifically the μ -opioid receptor (μOR). Opioids bind to μOR via N-chain orientation, where the phenethyl group is oriented towards the interior of the μOR (Figure 4).²² The activity of fentanyl is closely related to the presence of this phenethyl group, as norfentanyl, the inactive metabolite of fentanyl, lacks this phenethyl group.

A study conducted by Ling et al. concerned the use of a rhodium porphyrin, tetra(*p*-sulfonatophenyl) porphyrin Rhodium (III) [(TSPP)Rh(III)] found that the *N*-dealkylation of tertiary amines occurs in acidic, aerobic conditions at 80°C.²³ The proposed mechanism for the metalloporphyrin-assisted *N*-dealkylation is as follows: **a**: coordination of metal center to tertiary amine; **b**: β -hydride elimination resulting in the formation of an iminium ion and (TSPP)Rh(I); **c**: hydrolysis of iminium ion resulting in the formation of a secondary amine and a carbonyl; **d**: reduction of (TSPP)Rh(I) to

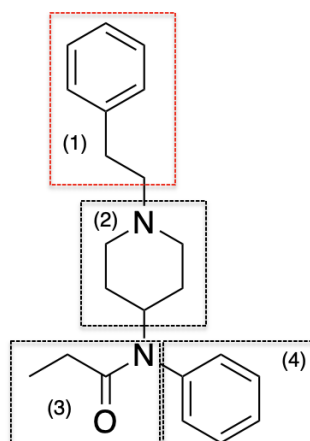
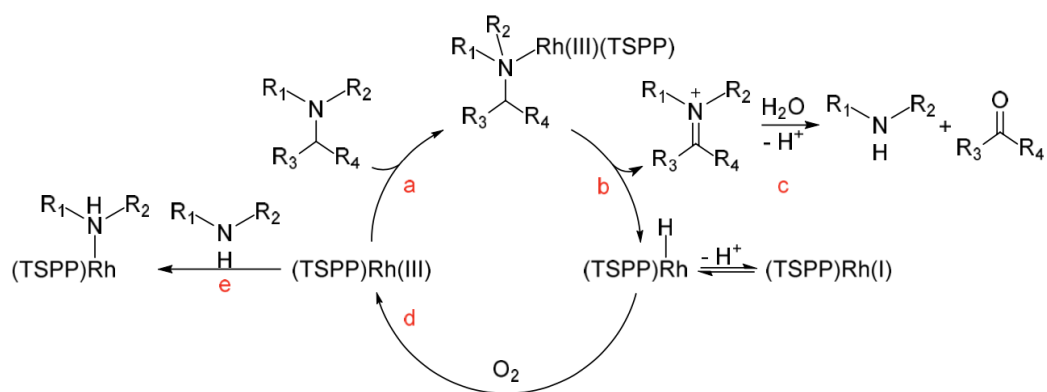


Figure 4. Structure of fentanyl; (1): phenethyl ring, (2): piperidine ring, (3) carbamide, (4): phenyl ring.



Scheme 1. Proposed mechanism for the *N*-dealkylation of tertiary amines by (TSPP)Rh(III).

(TSPP)Rh(III); e: binding of secondary amine to (TSPP)Rh(III), resulting in poisoning of catalyst (Figure 5). Ling et al. introduced acid to the reaction to prevent the poisoning of the acid by the secondary amine. As demonstrated by this research, metalloporphyrins are a promising potential catalyst for the degradation of fentanyl.

1.6 Hypothesis and Overview of Experimental Objectives

The presence of tertiary amines in fentanyl makes it a promising target for potential catalysts. As demonstrated by Ling *et al.*, metalloporphyrin complexes serve as effective catalysts for the *N*-dealkylation of tertiary amines. As such, it is proposed that a water-soluble porphyrin similar to [(TSPP)Rh(III)] can be employed to degrade fentanyl via an oxidative *N*-dealkylation pathway.

The scientific goals of this project are to (a) prepare a water-soluble iron porphyrin complex, tetra(*p*-sulfonatophenyl) porphyrin iron (III) [(TSPP)Fe(III)] (**9**) (Figure 5), for the selective degradation of fentanyl and (b) to monitor the degradation of fentanyl in aqueous solutions at 37 °C with time-of-flight mass spectrometry (TOFMS). The aim of this research is to develop a biocompatible catalyst for the rapid degradation of fentanyl that would not need to interact with existing opioid receptors in the body.

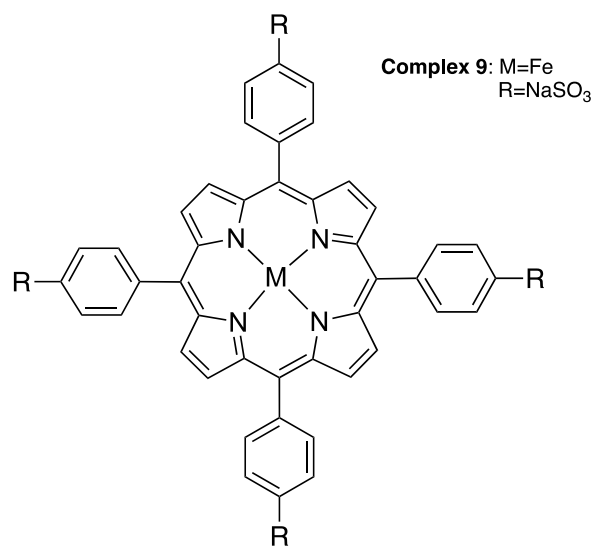


Figure 5. General structure of water-soluble metalloporphyrin.

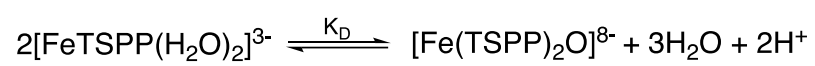
It was hypothesized that a porphyrin with an iron metal center, similar to the active site in CYP 3A4, would degrade fentanyl in aqueous solutions via an oxidative *N*-dealkylation pathway. In Chapter 2, the synthesis and purification of complex **9** is outlined. Additionally, the ability of complex **9** to effectively degrade fentanyl in aqueous solutions at varying concentration was explored.

Chapter 2 Degradation of Fentanyl Using Tetra(*p*-sulfonatophenyl)porphyrin Iron (III)

2.1 Introduction

The catalyst in this research, tetra(*p*-sulfonatophenyl)porphyrin iron (III) [(TSPP)Fe(III)] (**9**), is a commercially available, water-soluble metal catalyst, with a broad range of applicability. It has low toxicity, high stability, and high oxidation potential for many substrates.²⁴ Much of the research surrounding complex **9** involves studying its use as a biomimetic catalyst due to its similarity to heme and its high solubility in water. Porphyrins typically are immiscible in water, however, the presence of the polar sulfonic acid substituents in TSPP results in the complex having high water solubility.

Complex **9** was first synthesized as a sodium salt and characterized by Fleischer et al. in 1971.²⁵ The synthesis involved refluxing the free-base porphyrin with FeSO₄·7H₂O in water. Complex **9** has also been synthesized by reacting the free-base porphyrin and FeCl₂·4H₂O in refluxing dimethylformamide (DMF).²⁶ A pH-dependent equilibrium exists in aqueous solutions which results in the formation of a monomeric form and a dimeric form (Scheme 2).²⁴ The formation of the monomeric form is favored in acidic media, whereas the formation of the dimeric form is favored in basic media. The dimeric form exists as the μ -oxo-bridged dimer. The two forms can be differentiated using UV-Vis spectroscopy. The two forms can be differentiated using UV-Vis spectroscopy. The spectrum of monomer displays a Soret band between



Scheme 2. Equilibrium of monomeric and dimeric forms of FeTSPP.

392 and 395 nm and two Q bands at 528 nm and 680 nm. The dimer has a Soret band between 410 and 415 nm and two Q bands at 565 nm and 606 nm.²⁴

Complex **9** has been shown to have broad catalytic applicability with regard to oxidation reactions. Typically, hydrogen peroxide is used as the oxidizing agent. The mechanism of this reaction was proposed by Lente et al. and consists of complex **9** forming a reactive iron-hydroperoxo-complex when in the presence of hydrogen peroxide. Subsequently, an iron(IV)-oxo-species is formed in lower amounts.²⁷ Vakuliuk et al. reported the chemoselective aerobic oxidation of *trans*-anethol producing the allylic aldehyde only in the presence of complex **9** molecular oxygen. When complex **9** is replaced by a peroxidase, *para*-anisaldehyde is the major product, in addition, the 1,6 diol is obtained. This suggests that the FeTSPP catalyzed reaction is chemoselective.²⁸

Meunier et al. attempted to catalyze the epoxidation of styrene and the hydroxylation of ethyl benzene using the tetrasodium salt of FeTSPP (FeTSPPNa). It was found that FeTSPPNa was unable to catalyze either reaction. Meunier et al. then embedded FeTSPPNa in polymers with highly branched, multi-armed chains of polypeptides. This was done to simulate the hydrophobic environment surrounding the active site in CYP 3A4. The reactions proceeded successfully, with TON values of 8500 for the epoxidation reaction and 3800 for the hydroxylation, with yields 97% and 92% respectively (Figure 6). The pH range of the polymer remained between 4-10 with the porphyrin bound in the polymer, suppressing mostly dimer formation.

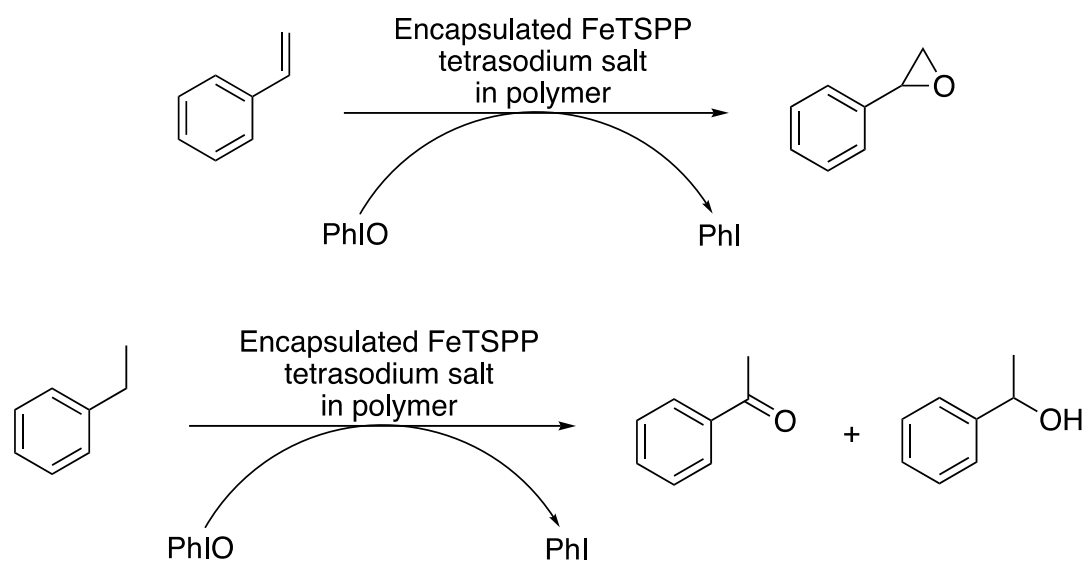


Figure 6. FeTSPP catalyzed epoxidation and hydroxylation.

The porphyrin was able to be released from the polymer and recycled at pH > 12.²⁹

FeTSPP has been shown to have applications for industrial processes. FeTSPP has been employed as a biomimetic ligninase capable of degrading lignan-model compounds.²⁴ The degradation of lignan is important in the industrial manufacturing of paper. Another application of FeTSPP has been in the degradation of environmental pollutants. Meunier et al. studied the oxidative degradation of organic halides, such as 2,4,6-trichlorophenol, in the presence of FeTSPP and an oxidizing agent (hydrogen peroxide or potassium monosulfate). 2,4,6-trichlorophenol is an example of an anthropogenic pollutant, which are pollutants that are unable to be degraded by microorganisms and bioaccumulate in the tissues of plants and animals. It was discovered that 2,4,6-trichlorophenol formed the corresponding chinone via oxidative dichlorination, with potassium monopersulfate producing the chinone in higher yield.³⁰

FeTSPP is a commercially available compound on the milligram or gram scale and has been shown to be an effective oxidation catalyst with biomimetic properties. Catalytic studies with FeTSPP can be run in the presence of peroxides, such as hydrogen peroxide, or molecular oxygen. Future work for this catalyst involves improving catalyst recycling and catalyst loading.²⁴

2.2 Results

2.2.1 Synthesis and Characterization of Iron (III) Porphyrins

A water-soluble porphyrin complex with an iron metal center was synthesized and purified (**9**) according to procedures outlined in literature.^{25,26} Two separate synthetic and purification methods were used, and the separate complexes will be denoted as **9a** and **9b**. The resulting products were characterized using UV-Vis spectroscopy. The UV-Vis spectrum for complex **9a** shows a Soret band with a λ_{max} at 394 nm ($\epsilon_{394 \text{ nm}} = 303,925 \text{ M}^{-1} \text{ cm}^{-1}$) and a Q band at 528 nm (Figure 7). The resulting UV-Vis spectrum of complex **9b** shows a Soret band with a λ_{max} at 394 nm ($\epsilon_{394 \text{ nm}} = 99,015 \text{ M}^{-1} \text{ cm}^{-1}$), which suggests successful metalation of the free-porphyrin (Figure 9).

2.2.2 Degradation of Fentanyl in Aqueous Solutions Using Complex **9a**

To determine the efficacy of **9a** with regards to the degradation of fentanyl, several reactions were prepared with 10 μM fentanyl solution and varying concentrations of **9a** (10 μM – 50 μM). The reactions were stirred and incubated at 37°C in glass vials. Small aliquots were retrieved from the vials at time points 0, 2h, 4h, 6h, 24h, 48h, and 72 h. The breakdown of fentanyl was monitored using TOFMS. Control reactions, in which either fentanyl or **9a** is absent, were also performed. The amount of fentanyl present in solution after each time point was determined from extracted ion chromatograms, where the change in peak area of fentanyl over time was measured. Figure 11 displays the % fentanyl remaining in solution after each time point, as well as the ratio of catalyst to substrate present at each time point.

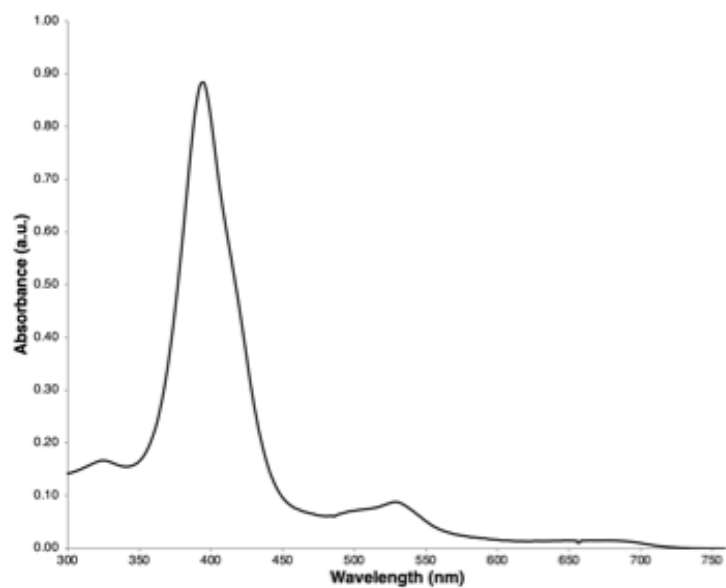


Figure 7. UV-visible spectrum of **9a**.

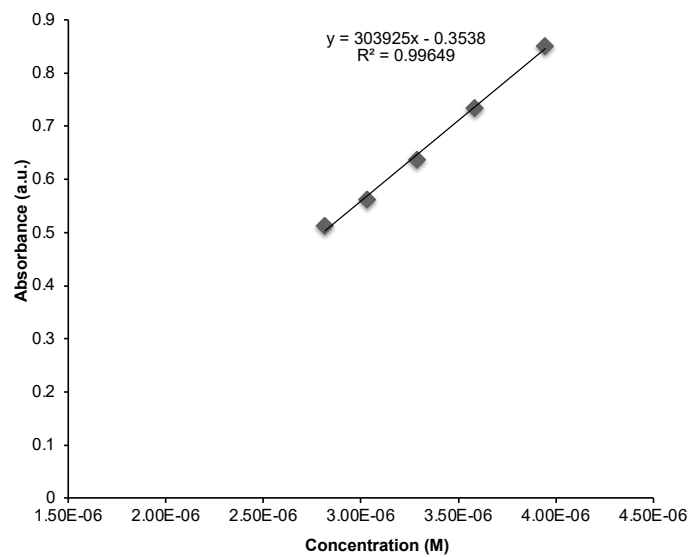


Figure 8. Calibration plot of **9a** following purification on ion-exchange column.

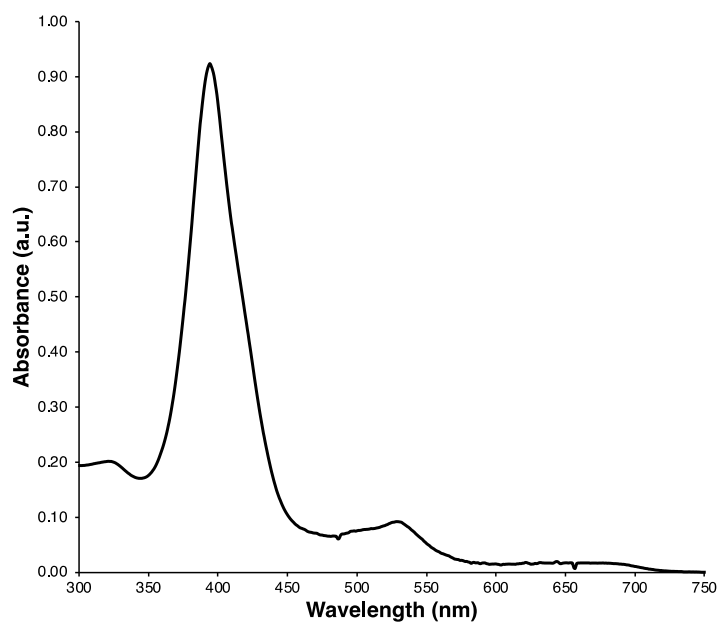


Figure 9. UV-visible spectrum of **9b**.

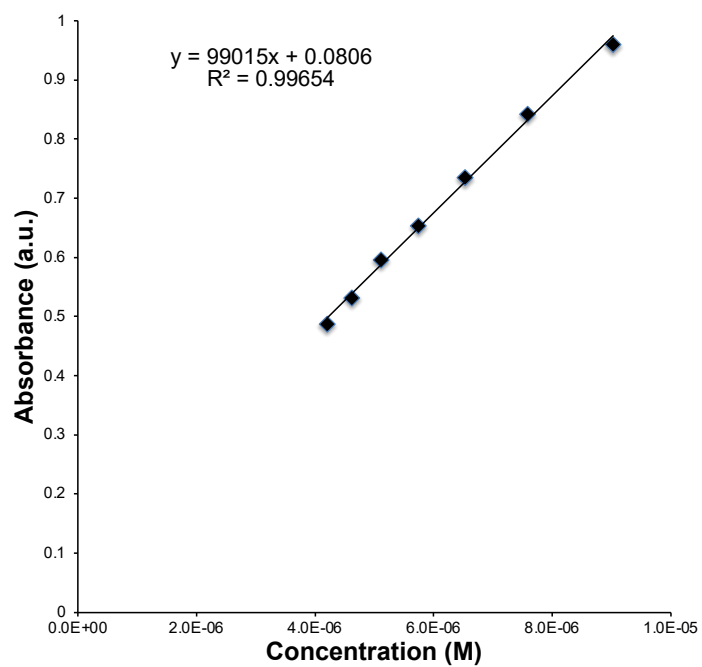


Figure 10. Calibration plot of **9b** following purification on Sephadex column.

Breakdown products were observed, and their proposed structures are shown in Figure 12. Additionally, their mass-to-charge ratios were identified and are shown in Table 1.

*2.2.3 Degradation of Fentanyl in Aqueous Solutions Using Complex **9b***

To determine the efficacy of **9b** with regards to the degradation of fentanyl, several reactions were prepared with 10 μM fentanyl solution and varying concentrations of **9b** (10 μM – 50 μM). The reactions were stirred and incubated at 37°C in glass vials. Small aliquots were retrieved from the vials at time points 0, 2h, 4h, 6h, 24h, 48h, and 72 h. The breakdown of fentanyl was monitored using TOFMS. Control reactions, in which either fentanyl or **9b** is absent, were also performed. The amount of fentanyl present in solution after each time point was determined from extracted ion chromatograms, where the change in peak area of fentanyl over time was measured. Figure 13 displays the % fentanyl remaining in solution after each time point, as well as the ratio of catalyst to substrate present at each time point. No breakdown products were observed.

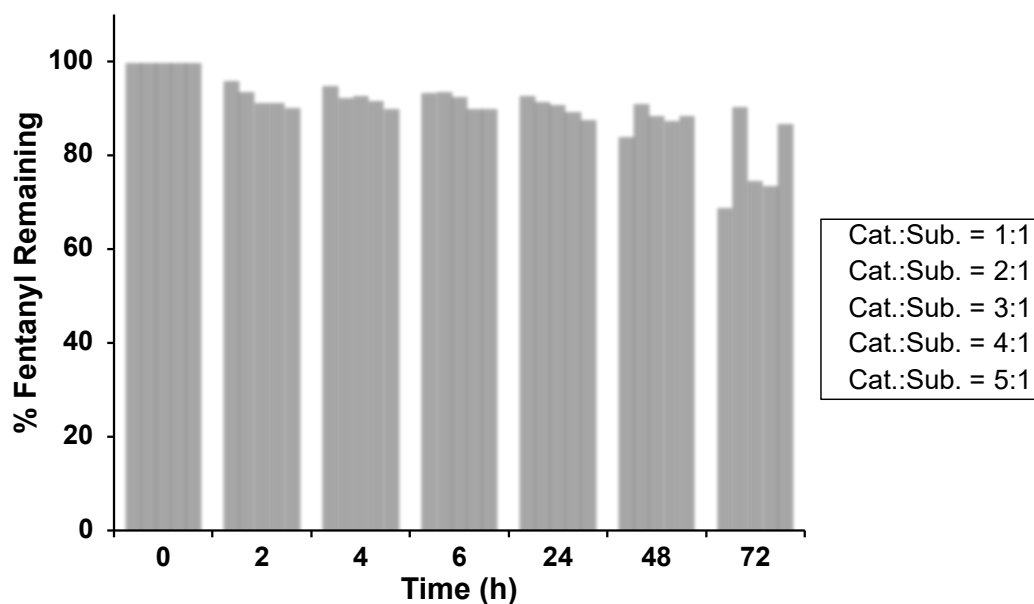


Figure 11. Change in fentanyl peak area at varying catalyst substrate ratios from time 0 to 72 hours, using complex **9a**.

Table 1. Products observed following breakdown of fentanyl using complex **9a**.

Retention Time (min)	m/z
3.730	233.164
3.938	132.045
5.605	187.124

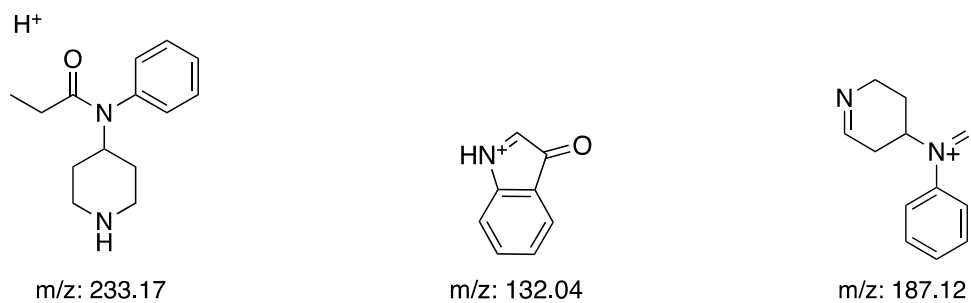


Figure 12. Proposed breakdown products for the degradation of fentanyl in aqueous solutions.

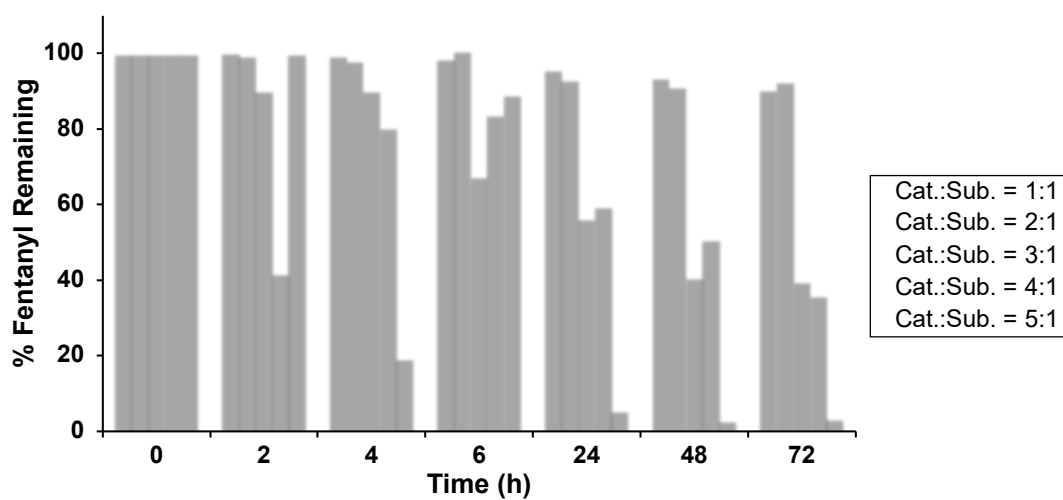


Figure 13. Change in fentanyl peak area at varying catalyst substrate ratios from time 0 to 72 hours, using complex **9b**.

2.3 Discussion

2.3.1 Characterization and Purification of Iron Porphyrin Complexes

Successful metalation of the free-base porphyrin was determined using UV-visible spectroscopy. The UV-visible spectrum of the free-base porphyrin, tetra(*p*-sulfonatophenyl) porphyrin, shows a soret band with λ_{max} at 413 nm. The UV-visible spectra of complexes **9a** and **9b** each display a soret band with λ_{max} at 394 nm, consistent with literature values reported for the complex. Therefore, the metalation of the free-base porphyrin with iron was deemed successful.

Complexes **9a** and **9b** were prepared using two different synthetic schemes and two different purification methods. Complex **9a** was purified using an ion-exchange column and complex **9b** was purified on Sephadex, a size-exclusion chromatography. The extinction coefficient value, ϵ , obtained for complex **9a** was $303,925 \text{ M}^{-1} \text{ cm}^{-1}$, which was much higher than the reported literature value. It is believed that the high extinction coefficient value of complex **9a** was due to the presence of free-base porphyrin in the sample. Complex **9b** was found to have an extinction coefficient value of $99,015 \text{ M}^{-1} \text{ cm}^{-1}$, which is still larger than the reported literature value of $24,000 \text{ M}^{-1} \text{ cm}^{-1}$ but closer to the expected value.

2.3.2 Removal of Fentanyl Using Complex **9a**

Complex **9a** did not degrade fentanyl in aqueous solutions as effectively as hypothesized. A concentration of $10 \text{ }\mu\text{M}$ of catalyst yielded the best results, with

30.75% of fentanyl disappearing from aqueous solution after 72 hours. These results could be explained by the questionable purity of the complex. Breakdown products were observed, and their proposed structures are shown in Figure 12. One of the breakdown products is norfentanyl (**2**), which results from the *N*-dealkylation of the tertiary amine. The identities of all observed breakdown products have not been identified.

2.3.3 Removal of Fentanyl Using Complex **9b**

The degradation of fentanyl was measured in the presence of complex **9b**. It was found that complex **9b** appeared to be a more effective catalyst at higher concentrations, with 96.71% removal of fentanyl from aqueous solutions after 72 hours with a catalyst concentration of 50 μ M. However, no breakdown products were observed for these reactions, so it is not known whether fentanyl was converted to its inactive nor metabolite in the presence of complex **9b**.

2.4 Conclusions

The aim of this research was to develop an iron porphyrin complex capable of degrading fentanyl via a catalytic oxidative *N*-dealkylation pathway. The synthesis and purification of iron (III) tetra(*p*-sulfonatophenyl) porphyrin were explored. Complex **9a** demonstrated a slight ability to degrade fentanyl in aqueous solutions, with 30.75% removal of fentanyl after 72 hours. Mass spectral analysis of the breakdown products suggests the mechanism proceeds via an oxidative *N*-dealkylation

of the tertiary amine present in the piperidine ring, producing norfentanyl, an inactive metabolite of fentanyl.

Complex **9b** was synthesized and purified using different synthetic and purification schemes in order to optimize purity of the porphyrin complex. It was found that fentanyl showed greater disappearance from aqueous solutions in the presence of complex **9b**. There were no breakdown products observed for those reactions, so the mechanism for the breakdown of fentanyl cannot be ascertained for those reactions.

2.5 Materials and Methods

2.5.1 General Data

UV-visible absorption spectra were recorded at 25 °C on an HP 8463 diode array spectrometer in 1 cm quartz cuvettes. High-resolution mass spectra were recorded on an Agilent 6560 IM-QTOF. All measurements were made in nitrogen drift gas maintained at approximately 4 Torr and 25 °C.

Reagents and solvents were obtained as follows and used as received: meso-tetra(4-sulfonatophenyl) porphine dihydrochloride S₄TPP (Frontier Scientific), meso-tetra(4-sulfonatophenyl) porphine tetrasodium salt dodecahydrate (Frontier Scientific), FeSO₄·7H₂O (Fisher Scientific), anhydrous DMF (Acros Organics), acetone (VWR), diethyl ether (VWR), Dowex 50WX8-100 ion-exchange resin (Sigma Aldrich), Sephadex G-10 (Cytiva), FeCl₂·4H₂O (Flinn Scientific). For LC-MS the solvent used

was water (Optima LC-MS grade Fisher Scientific). Cation-exchange column and Sephadex column were performed using Millipore Direct-Q 18.2 M Ω H₂O.

2.5.2 Synthesis of (TSPP)Fe(III) (**9a**)

A 500 mL round bottom flask was charged with H₂TPPS (0.0816 g, 0.0659 mmol), water (100 mL), and FeSO₄ (0.0739 g, 0.2658 mmol). The solution was refluxed for 30 minutes and then cooled. The solution was dried under vacuum. Water (2 mL) was added to the dried sample and passed through Sephadex G-10 (5.051 g) using Millipore water as eluent. The solution was reduced under vacuum. Further purification was accomplished by precipitation of the FeTPPS from solution by the addition of acetone (12 mL) and washed with acetone (3 x 10 mL) and diethyl ether (3 x 4 mL). Dark red solid, crude yield 0.0687 g, UV-VIS: (H₂O) [λ_{\max} , nm (ϵ , M⁻¹ cm⁻¹): 394 (303925)].

2.5.3 Synthesis of (TSPP)Fe(III) (**9b**)

A 250 mL round bottom flask was charged with anhydrous DMF (25 mL) and refluxed. H₂TPPS (0.0534 g, 0.0431 mmol) was added to the flask and allowed to dissolve (ca. 3 min). FeCl₂ (0.0739 g, 0.266 mmol) was added to the flask and the solution was refluxed for 30 minutes and then cooled. Two volumes of toluene were added to the solution and the solvent was removed using a rotary evaporator. Water (2 mL) was added to the dried sample and passed through Sephadex G-10 (10.020 g) using water. The solution was reduced using a rotary evaporator. Further purification

was accomplished by precipitation of the FeTPPS from solution by the addition of acetone (12 mL) and washed with acetone (3 x 10 mL) and diethyl ether (3 x 4 mL). Red/brown solid, crude yield 0.0354 g, UV-VIS: (H₂O) [λ_{max} , nm (ϵ , M⁻¹ cm⁻¹): 394 (99015)].

*2.5.4 Degradation Studies Performed with Complex **9a***

A stock solution of fentanyl (0.001g, 0.60 mmol) was prepared by adding optima grade LC-MS water (3.953 mL) to the 1 mg/mL solution of fentanyl in methanol. A stock solution of **1** (0.0054 g, 0.0042 mmol) was prepared in optima grade LC-MS water (8.500 mL). Stock solutions were kept at 37 °C for one hour before the start of the studies.

The study was performed at with five different **1**:fentanyl ratios, 1:1, 2:1, 3:1, 4:1, and 5:1. Aliquots were collected at seven time points (0h, 2h, 4h, 6h, 24h, 48h, 72h). Samples were quenched by freezing in liquid nitrogen.

*2.5.5 Degradation Studies Performed with Complex **9b***

A stock solution of fentanyl (0.001g, 0.60 mmol) was prepared by adding optima grade LC-MS water (3.953 mL) to the 1 mg/mL solution of fentanyl in methanol. A stock solution of **1** (0.0054 g, 0.0050 mmol) was prepared in optima grade LC-MS water (8.359 mL). Stock solutions were kept at 37 °C for one hour before the start of the studies.

The study was performed at with five different 1:fentanyl ratios, 1:1, 2:1, 3:1, 4:1, and 5:1. Aliquots were collected at seven time points (0h, 2h, 4h, 6h, 24h, 48h, 72h).

Samples were quenched by freezing in liquid nitrogen.

Conclusions

The aim of this work was to develop a water-soluble metalloporphyrin for the catalytic *N*-dealkylation of fentanyl in aqueous solutions. Complexes **9a** and **9b** were both shown to remove fentanyl from aqueous solutions at 37 °C. Complex **9a** removed 30.75% of fentanyl from solution with a catalyst concentration of 50 μM. In the presence of complex **9b**, 96.71% of fentanyl disappeared from solution after 72 hours with a catalyst concentration of 50 μM.

Three breakdown products were observed following the reaction between fentanyl and complex **9a**. Most notably, norfentanyl, an inactive fentanyl metabolite, was identified as a product. The formation of norfentanyl suggests the mechanism proceeded via an *N*-dealkylation pathway. There were no breakdown products observed following the reaction between fentanyl and complex **9b**.

Overall, complex **9** demonstrated ability to degrade fentanyl in solution but did not perform as effectively as hypothesized. This could be due to the purity of the complex. The breakdown products observed support the suspected mechanism of *N*-dealkylation of fentanyl at the piperidine ring.

Future Work

Fentanyl has been shown to degrade in aqueous solutions in the presence of complex **9a**, however the rate of disappearance was not as efficient as hypothesized. The catalytic reactions were performed in open air, relying on the oxygen from the air to serve as an oxidizing agent. The use of alternate oxidizing agents, such as hydrogen peroxide or molecular oxygen, need to be explored to investigate if the oxidizing agent has any significant effect on catalytic activity.

Additionally, as suggest by UV-Vis spectroscopic evidence, the purity of complex **9a** is questionable. Therefore, alternate purification methods of complex **9a** need to be explored. Future work could involve exploring the purification of complex **9a** using reverse-phase HPLC as opposed to column chromatography.

Furthermore, the use of complex **9a** as a catalyst for the *N*-dealkylation of other tertiary amines will need to be explored. Research into the *N*-dealkylation of amines has value in both biology and synthetic chemistry, with resulting products having applications in pharmaceuticals and fine chemicals.

References

1. Brownstein, M.J. *Proc. Natl. Acad. Sci. USA*. **1993**, *90*, 5391-5393.
2. Heslop, D.J.; Blain, P.G. *Intelligence and National Security*. **2020**, *35(4)*, 539-555.
3. Overdose Death Rates. <https://nida.nih.gov/drug-topics/trends-statistics/overdose-death-rates>, **2022**.
4. Qi, L.; Cheng, Z.; Zuo, G.; Li, S.; Fan, Q. *Defense Science Journal*. **2011**, *61*, 30-35.
5. Pal, H.; Nina, A.; Nag, O.; Chouinard, C.; Pitt, A.; Ellis, G.A.; Walper, S.A.; Deschamps, J.; Burkus-Matesevac, A.; Maiello, K.; Delehanty, J.B.; Knight, D.A. *J. Inorg. Bio*. **2022**, 235.
6. Riches, J.R.; Read, R.W.; Black, R.M.; Cooper, N.J.; Timperley, C.M. *J. Anal. Toxicology*. **2016**, *36*, 647-656.
7. Nakagaki, S.; Ferreira, G.K.B.; Ucoski, G.M.; Dias de Frietas Castro, K.A. *Molecules*. **2013**, *18*, 7279-7308.
8. Scott, E.E.; Halpert, J.R.; *TRENDS in Biochemical Science*. **2005**, 30.
9. Sevrioukova, I.F.; Poulos, T.L. *Dalton Trans*. **2013**, *42(9)*, 3116-3126.
10. Girvan, H.M.; Munro, A.W. *Curr. Opin. Chem. Biol.*. **2016**, *13*, 136-145.
11. Labroo, R.B.; Paine, M.F.; Thummel, K.E.; Kharasch, E.D. *Drug Metab. Dispos*. **1997**, *25(9)*, 1072-1080.
12. Pereira, M.M.; Dias, L.D.; Calvete, M.J.F. *ACS Catal*. **2018**, *8*, 10784-10808.

13. Garg, A.; Solas, D.W.; Takahashi, L.H.; Cassella, J.V. *J. Pharma. Biomed.* **2010**, *53*, 325-334.
14. Trawiński, J.; Szpot, P.; Zawadzki, M.; Skibiński, R. *Sci. Total Environ.* **2021**, *791*.
15. Najmi, A.A.; Bischoff, R.; Permentier, H.P. *Molecules.* **2022**, *27*, 3293.
16. Murahashi, S.I.; Watanabe, T.; *J. Am. Chem. Soc.* **1979**, *101*, 7429-7230.
17. Carroll, R.J.; Leisch, H.; Scocchera, E.; Hudlicky, T.; Cox, D.P. *Adv. Synth. Catal.* **2008**, *350*, 2894-2992.
18. Santa, T.; Miyata, N.; Hirobe, M. *Chem. Pharm. Bull.* **1984**, *32*, 1252-1255.
19. Do Pham, D.D.; Kelso, G.F.; Yang, Y.; Hearn, M.T.W.W. *Green Chem.* **2012**, *14*, 1189-1195.
20. Dong, Z.; Scammels, P.J. *J. Org. Chem.* **2007**, *72*, 9881-9885.
21. Wang, S.; Yang, J.; Li, D.; Yang, J. *Eur. J. Org. Chem.* **2021**, *2021*, 6768-6772.
22. Lipiński, P.F.J.; Kosson, P.; Matalińska, J.; Roszkowski, P.; Czarnocki, Z.; Jarończyk, M.; Misicka, A.; Dobrowolski, J.C.; Sadlej, J. *Molecules.* **2019**, *24*, 740-440.
23. Ling, Z.; Yun, L.; Liu, L.; Wu, B.; Fu, X. *Chem. Commun.* **2013**, *49*, 4214.
24. Böhm, P.; Gröger, H. *Chem. Cat. Chem.* **2015**, *7*, 22-28.
25. Fleischer, E.B.; Palmer, J.M.; Srivastava, T.S.; Chatterjee, A. *J. Am. Chem Soc.* **1971**, *93*, 3162-3167.

26. Halma, M.; Dias de Freitas Castro, K.A.; Prévot, V.; Forano, C.; Wypych, F.; Nagasaki, S. *J. Mol. Catal. A Chem.*, **2009**, *310*, 42-50.
27. Lente, G.; Fábíán, I. *Dalton Trans.* **2007**, 4268-4275.
28. Vakuliuk, O.; Mutti, F.G.; Lara, M.; Gryko, D.T.; Kroutil, W. *Tetrahedron Lett.* **2011**, *52*, 3555-3557.
29. Meunier, B.; Robert, A.; Pratviel, G.; Bernadou, J. *The Porphyrin Handbook*, 4 (Eds. Kadish, K.M.; Smith, K.M.; Guillard, R.) Academic Press, New York, **2000**.
30. Meunier, B.; Belal, R.; Momenteau, A.; Labat, G. *Chim. Ind.* **1990**, *72*, 433-440.